World Scientific Research Journal (WSRJ) ISSN: 2472-3703
www.wsr-j.org

Influence of Small Scale Heterogeneity on multiphase flow particles

Zheng He, Xuan Gu[a, *], Xiaoyu Sun, Jianxin Teng, YingShu Pang

College of Aerospace and Civil Engineering, Harbin Engineering University, Harbin

150001 China

[a]guxuan@hrbeu.edu.cn

Abstract: Here we provide a comprehensive study of the fundamental physics both numerically and analytically, of the combined influence of heterogeneity, viscous forces, gravity, and capillarity on multiphase flow of CO2 and brine. Specifically, steady-state 3D core flood displacements in heterogeneous cores over a range of relevant conditions are simulated to study the impact of sub-core heterogeneity on CO2/brine displacements over a wide range of flowrates. Various degrees of heterogeneity are generated based on the normal random distribution as well as for real models of cores based on 3D X-Ray tomography. A 2D semi-analytical model considering gravity and permeability heterogeneity is developed for predicting brine displacement efficiency over a wide range of capillary numbers that provides good agreement with the simulated 3D results. The analytical derivation is general, and the provided solution can estimate the flow regimes for horizontal core floods efficiently.
Keywords: Heterogeneity, Capillarity, Immiscible flow, CO2 sequestration.

---

1. INTRODUCTION

Rock heterogeneity is ubiquitous in geological formation and exists at every scale: pore-scale (~μm), grain scale (~mm), core-scale (~0.1 to 10 cm), and field-scale (~10 cm and larger). These different scales of heterogeneity result in complexity when solving multiphase flow problems. For example, a typical experimental CO_2 saturation distribution inside a Berea Sandstone rock sample is shown in Fig. 1. This saturation distribution was measured while a mixture of CO_2 (95%) and brine (5%) were injected into the core and after the saturation distribution was no longer changing [1]. It is shown that the sub-core scale heterogeneity can affect the saturation significantly. One interesting and important feature of the experiment is that capillary barrier results in a large portion of the core near the outlet end that is almost completely bypassed by the CO_2, which indicates capillary barriers within the rock can affect flow behavior significantly. If the orientation of a capillary barrier is perpendicular to the flow direction, the non-wetting phase fluid in a water-wet system may be trapped inside high permeability zones surrounded by low permeability ones[2-4]. It has also been suggested that

capillary heterogeneity provides a new trapping mechanism in carbon sequestration [5] in addition to structural trapping, residual trapping, dissolution trapping and mineral trapping. Therefore, in this work, we are focused on understanding the influence of spatial heterogeneity at the sub-core scale (~1 mm^3) on multiphase flow of $CO_2$and brine.

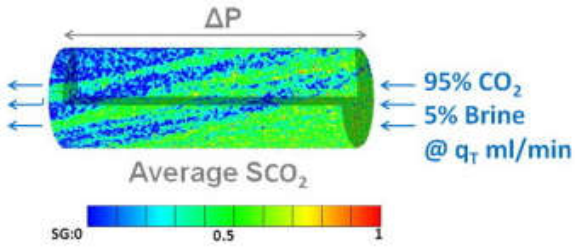

Fig. 1 The experimental steady state three-dimensional views of CO_2 saturation in the core for a given fractional flow of CO_2 at a given flow rate. The fluids were injected from right to left [1].

In a recent study [6], the combined effect of viscous, gravitational, and capillary forces at the core-scale has been studied numerically and analytically for homogeneous cores. The major points can be seen in Fig. 2, where a series of calculated average CO_2 saturations for three different permeability cores are plotted as a function of gravity number N_{gv} and Bond number N_B. Gravity number N_{gv} measures the balance between gravity and viscous forces while Bond number N_B is a ratio of gravity to capillary force.

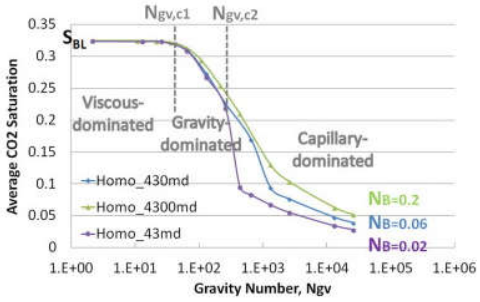

Fig. 2 Average CO_2 saturation as a function of gravity number N_{gv} for the homogeneous cores with three different values of effective permeability (k = 4300, 430, and 43 md) and their corresponding Bond numbers (N_B = 0.2, 0.06, 0.02) (from [6]. The interfacial tension σ is kept as a constant, 22.47 mN/m.

2. METHODOLOGY OF RESEARCH

A detailed description of the methodology for numerical simulations performed in this study can be found in Kuo and Benson [6] and Kuo et al. [7]. Here we briefly highlight some important features. First, TOUGH2-MP/ECO2N[8-11] is used for the numerical simulations. Grid refinement studies were carried to ensure that grid resolution was sufficiently small to avoid numerical artifacts. In addition, to avoid numerical artifacts caused by the time-step size,

the initial time step is chosen to have a small CFL number ($u_x\Delta t/\Delta x < 1$) for every flow rate, for example, 0.04–0.3. For subsequent time steps, it is automatically adjusted by TOUGH2 to higher or lower values during a simulation run dependent on the convergence rate. After breakthrough, the time step size will increase up to the maximum time step size Δt_{max} set up at the beginning.

We use the same modified J-function and the same fitting parameters of the J-function as in the previous paper [6]. The core is assumed to be strongly water wet, hence the contact angle $\theta = 0$ is used in the simulation. Note that the entry capillary pressure is zero in this work. Based on the Leverett scaling, constant porosity and permeability values for the homogeneous cores result in a uniform capillary pressure ($P_{c,mean}$) assigned to each grid cell while a unique pair of porosity and permeability values for the heterogeneous cores results in a range of capillary pressure curves within the boundary between $P_{c,max}$ and $P_{c,min}$(Fig. 3). These capillary pressure curves are a function of core heterogeneity. A higher degree of heterogeneity will result in a wider range of saturations [7]; [12] ; [13].

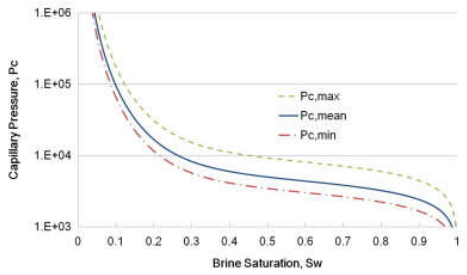

Fig. 3 A typical range of capillary pressure curves in the simulations, illustrating the mean capillary pressure curve ($P_{c,\ mean}$) and the bounds in the heterogeneous core.

Fig. 4 illustrates both the slice-average permeability and the corresponding steady-state average saturation (at the 6 ml/min total injection rate where the conventional capillary number $Ca = u_t\mu_{CO2}/\sigma$ is about 10^{-7}) along the flow direction for four random distributions.

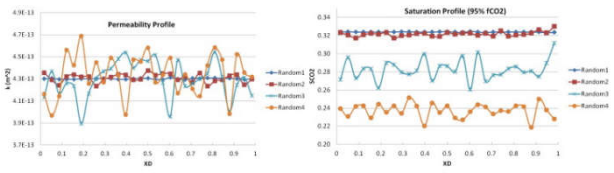

Fig. 4 Random Permeability Distribution: Four different random permeability profiles and the Corresponding average CO_2 saturations in the viscous-dominated regime. $x_D = x/L$ is the dimensionless coordinates in the x direction. $x_D = 0$ is the inlet end of the core while $x_D = 1$ is the outlet end.

Similarly, Fig. 5 illustrates the slice-averaged porosity profile and its two corresponding permeability profiles as well as the corresponding saturation profiles made at the small inverse capillary numbers (within the viscous dominated regime).

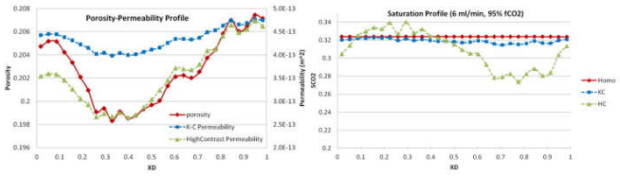

Fig. 5 (LHS) Porosity-based Permeability Distribution: Average porosity and two permeabilities (RHS) average CO_2 saturation along the flow direction for three different heterogeneous cores (homogeneous model, Kozeny–Carman model, and High Contrast model).

The simulation outputs (the average saturation in the core) of all the sensitivity cases will be analyzed in terms of dimensionless parameters (Fig. 6) such as traditional capillary number $Ca=u_t\mu_{CO2}/\sigma$, inverse capillary number N_{cv}, and gravity number N_{gv}. These dimensionless groups arise from the dimensional analysis of the continuum, macroscopic scale [6]. Each curve shown in Fig. 6 represents a sensitivity case with a constant Bond number (Table 5); flow rate is the only variable changing. The top figures are the simulation outputs analyzed in terms of Ca, while the middle figures are the same data analyzed in terms of N_{gv}.

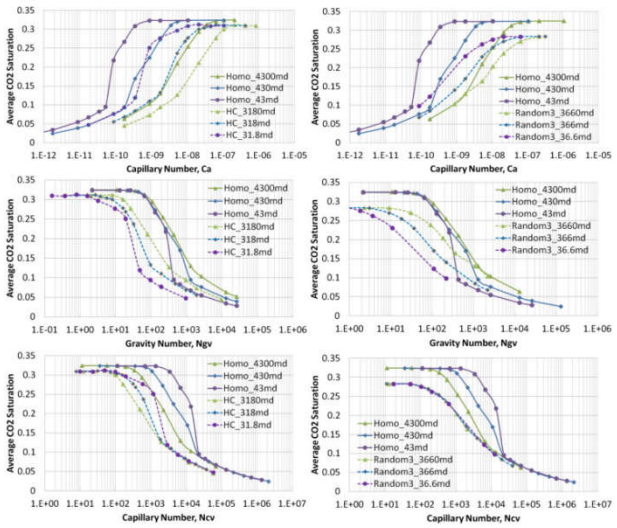

Fig. 6 Average CO_2 saturation as a function of traditional capillary number Ca, inverse capillary number N_{cv}, and gravity number N_{gv} for the two heterogeneous cores: High Contrast model (LHS) and Random 3 model (RHS). The interfacial tension σ is kept as a constant, 22.47 mN/m. Solid lines are used for homogeneous cores and dashed lines are used for heterogeneous cores.

All of the cases have the same simulation parameters, namely, relative permeability curves, capillary pressure curves, reservoir conditions, and grid size, etc. The only things changed are the permeability and/or porosity distribution of porous medium. Fig. 7 shows the average saturation for the two types of heterogeneous cores.

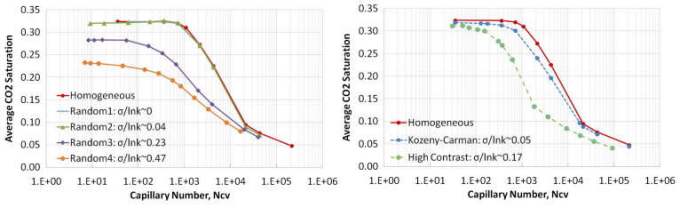

Fig. 7 Core average CO_2 saturation for the two types of cores over a wide range of capillary numbers N_{cv}. The interfacial tensions σ for all cases is 22.47 mN/m and the effective permeability varies from 254 to 570 md. The fractional flow of CO_2 is 95%.

Plotting the modified Buckley–Leverett solutions S_{BL}^{Hete} as a function of normalized standard deviation factor $\sigma_{lnk}/\ln(k_{eff})$ for random permeability cores can obtain a near-perfect linear correlation (LHS of Fig. 8).

$$S_{BL}^{Hete} = 0.324 - 0.1788\frac{\sigma_{lnk}}{\ln(k_{eff})} = \left(1 - 0.55185\frac{\sigma_{lnk}}{\ln(k_{eff})}\right)S_{BL}$$

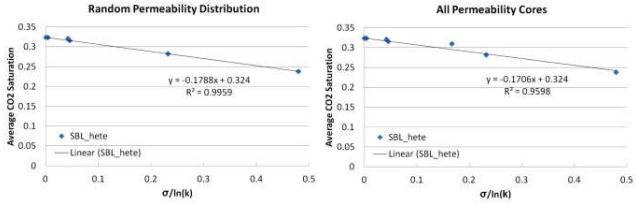

Fig. 8 Plotting the average CO_2 saturation, S_{BL}^{Hete}, as a function of normalized standard deviation factor$\sigma_{lnk}/\ln(k_{eff})$ for random permeability cores (LHS).

By adjusting these two values, the semi-analytical predictions agree with the simulation results quite well, with the exception of the capillary dominated regime for the random permeability core. Fig. 9 shows good agreement between the simulated results and the theoretical predictions for the average CO_2 saturations of base cases for the High Contrast model (LHS) and the Random 3 model (RHS), respectively.

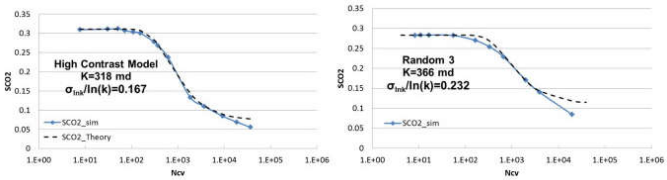

Fig. 9 Comparison of average CO_2 saturation as a function of capillary number N_{cv} between theoretical values and simulation results for the High Contrast model (LHS) and the Random 3 model (RHS).

Fig. 10 compares the simulation results and the predicted values for two models in a wide range of permeability. As shown, we can replicate the simulation results quite well. The prediction is even better for the random distribution core (Fig. 10b) for both permeability values. A slight mismatch observed at the High Contrast model ($0.1k$) is probably due to the

small Bond number ($N_B = 0.0165$) and the lack of information related to the correlated permeability distribution observed in the cores.

Fig. 11 shows the average CO_2 saturations of the High Contrast model as a function of capillary numbers for four different CO_2 fractional flows, 0.95, 0.79, 0.51 and 0.34. The heterogeneous factor τ stays constant for four cases since it is the same core.

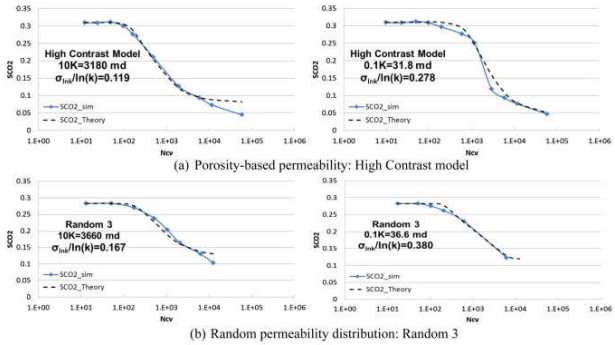

Fig. 10 Sensitivity studies of permeability for (a) High Contrast models and (b) Random 3 models.

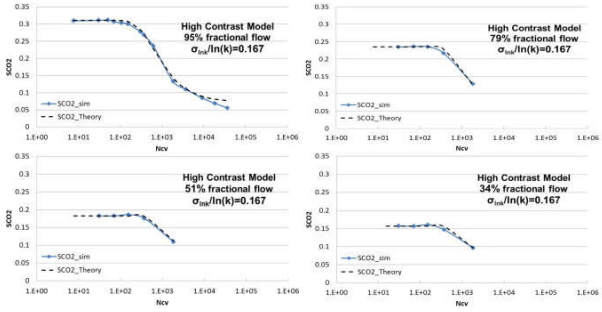

Fig. 11 Sensitivity studies of different fractional flows of CO_2 for High Contrast models (f_{CO2} = 95%, 79%, 51% and 34%).

One sensitivity study on the aspect ratio R_l is performed to test the semi-analytical model. The solution works well for the limited cases studied (Fig. 12). Since the input relative permeability curves and the fractional flow of CO_2(f_{CO2}=0.95) for this case are the same as for the base case of the High Contrast model, we can expect the modified Buckley–Leverett solution S_{lk}^{where} to remain the same.

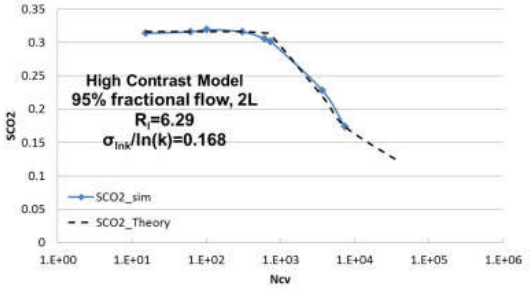

Fig. 12 Sensitivity studies of aspect ratio (R_l = 6.2890) for High Contrast models.

Fig. 13 shows the average CO_2 saturations as a function of capillary numbers for seven models. We use the semi-analytical solution for the homogeneous cores to predict cases with the small degree of heterogeneity (Fig. 13a) while the heterogeneous semi-analytical solution is used to predict cases with the large degree of heterogeneity (Fig. 13b).

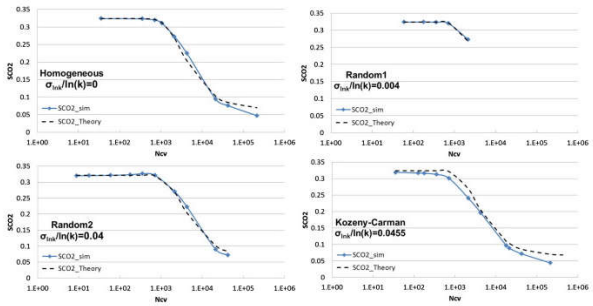

(a) Small degrees of heterogeneous cores ($\sigma_{lnk}/\ln k_{eff} < 0.05$)

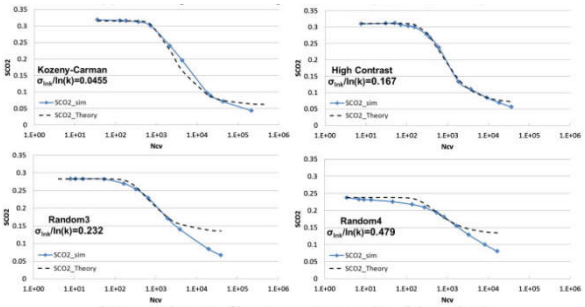

(b) Larger degrees of heterogeneous cores ($\sigma_{lnk}/\ln k_{eff} > 0.05$)

Fig. 13 Comparison of average CO_2 saturation as a function of capillary number N_{cv} between theoretical values and simulation results for sensitivity studies of (a) small degrees of heterogeneous cores and (b) large degrees of heterogeneous cores. Note that for very small amount of heterogeneity($\sigma lnk/\ln keff=0.004$), the results are nearly equal to the homogeneous core.

3. RESULTS AND DISCUSSION

The results shown in this work were mostly achieved with a specific core-shaped geometry and a limited number of permeability distribution. The heterogeneous porous medium is either based on a one specific rock or using a random log-normal distribution. The limitations inherent in the results are discussed in the following. First, if there are two systems with the same aspect ratio but the physical dimensions of the porous medium are meters instead of centimeters, the dimensionless plots which show the saturations are expected to be still valid. However, this needs to be confirmed with the large scale simulations.

Additionally, the results of specific distributions of permeability and a specific measure of heterogeneity should be qualitatively applied to a system, which is encountered different heterogeneity than what examined here. Therefore, to quantitatively predict the average saturation with different heterogeneity distributions, a systematic investigation on cores with various correlation lengths is needed to generalize and extend the analytical solution to a wider

range of rock types. Although we did not consider the correlation length and anisotropy in the derivation, it is not difficult to extend the derivation to include these two terms. Nevertheless, the "anisotropy" in the core is small because the ratio between the grid size in the x and z directions (which is the origin of the anisotropy) is about 3. This small amount of anisotropy is unlikely to have a large effect on the conclusions.

4. CONCLUTION

This paper addressed fundamental studies of multiphase flow of CO_2 and brine in heterogeneous porous media at the core-scale both numerically and analytically. The combined influence of gravity, flow rate and small-scale heterogeneity on core-scale multiphase flow of CO_2 and brine is an active and important research area needed to predict CO_2 storage efficiency in deep saline aquifers.

In this work, we developed and investigated new analytical techniques to study the balance of three forces as well as the sub-core heterogeneity in multiphase flow system. All the important parameters such as the degree of heterogeneity, gravity, size of the porous medium etc. are considered in the model. The solution has been compared with 3D high-resolution simulations to study the effects of viscous force, buoyancy force, capillary force as well as capillary heterogeneity on two-phase immiscible flow. The proposed 2D semi-analytical technique predicts the brine displacement efficiency for 3D two-phase flow simulations very well when the Bond number ranges from 0.02 to 0.2 and the degree of heterogeneity σ_{lnk}/ln k_{eff} smaller than 0.5. Theoretical predictions match the corresponding simulation results very well for all the sensitivity cases performed in this study.

ACKNOWLEDGEMENTS

This work is supported by the National Natural Science Foundation of China (o. 11602066) and the National Science Foundation of Heilongjiang Province of China (QC2015058 and 42400621-1-15047), the Fundamental Research Funds for the Central Universities.

EFERENCES

[1] J.-C. Perrin, M. Krause, C.-W. Kuo, L. Miljkovic, E. Charob, S.M. Benson Core-scale experimental study of relative permeability properties of CO2 and brine in reservoir rocks Energy Procedia, 1 (2009), pp. 3515–3522.

[2] Hamon G, Roy C. Influence of heterogeneity, wettability and coreflood design on relative permeability curves, SCA paper; 2000.

[3] M.M. Honarpour, A.S. Cullick Saad Naji, Humphreys NV. Effect of rock heterogeneity on relative permeability: implications for scale-up J. Pet. Technol., 47 (1995), pp. 980–986.

[4] G.E. Pickup, K.D. Stephen an assessment of steady-state scale-up for small-scale geological models Pet Geosci, 6 (2000), pp. 203–210.

[5] E. Saadatpoor, S.L. Bryant, K. Sepehrnoori New trapping mechanism in carbon sequestration Transp Porous Media, 82 (2010), pp. 3–17.

[6] C.-W. Kuo, S.M. Benson Analytical study of effects of flow rate, capillarity, and gravity on CO2/brine multiphase-flow system in horizontal core floods SPE J, 18 (4) (2013), pp. 708–720

[7] Kuo C-W, Perrin J-C, Benson S. Effect of gravity, flow rate, and small-scale heterogeneity on multiphase flow of CO2 and brine, SPE132607, SPE Western Regional Meeting, 27–29 May 2010, Anaheim, California, USA.

[8] Pruess K. ECO2N: A TOUGH2 fluid property module for mixtures of water, NaCl, and CO2, Lawrence Berkeley National Laboratory Report LBNL-57952, Berkeley, CA; 2005.

[9] Pruess K, Oldenburg C, Moridis G. TOUGH2 User's Guide, V2, Lawrence Berkeley National Laboratory Report LBNL-43134, Berkeley, CA, Advances In Water Resources, 1999; 29: p. 397–407.

[10] Zhang K, Wu YS, Ding C, Pruess K. TOUGH2_MP: a parallel version of TOUGH2. TOUGH symposium; 2003.

[11] K. Zhang, C. Doughty, Y.S. Wu, K. Pruess Efficient parallel simulation of CO2 geologic sequestration in saline aquifers SPE Reservoir Simulation Symposium, Houston, TX (2007).

[12] M. Krause, J.-C. Perrin, S.M. Benson Modeling permeability distributions in a sandstone core for history matching coreflood experiments SPE J, 16 (4) (2011).

[13] R. Pini, S.C.M. Krevor, S. Benson Capillary pressure and heterogeneity for the CO2/water system in sandstone rocks at reservoir conditions Adv Water Resour, 38 (2012), pp. 48–59.